

# Signatures of kinetic and magnetic helicity in the CMBR

Levon Pogosian

*Theoretical Physics, The Blackett Laboratory, Imperial College,  
Prince Consort Road, London SW7 2BZ, United Kingdom.*

Tanmay Vachaspati

*Department of Physics, Case Western Reserve University,  
10900 Euclid Avenue, Cleveland, OH 44106-7079, USA.*

Serge Winitzki

*Department of Physics and Astronomy, Tufts University, Medford, MA 02155, USA.*

P and CP violation in cosmology can be manifested as large-scale helical velocity flows in the ambient plasma and as primordial helical magnetic fields. We show that kinetic helicity at last scattering leads to temperature-polarization correlations ( $C_l^{TB}$  and  $C_l^{EB}$ ) in the cosmic microwave background radiation (CMBR) and calculate the magnitude of the effect. Helical primordial magnetic fields, expected from cosmic events such as electroweak baryogenesis, can lead to helical velocity flows and hence to non-vanishing correlations of the temperature and B-type polarization. However we show that the magnitude of the induced helical flow is unobservably small because the helical component of a magnetic field is almost force-free. We discuss an alternate scheme for extracting the helicity of a stochastically homogeneous and isotropic primordial magnetic field using observations of the CMBR. The scheme involves constructing Faraday rotation measure maps of the CMBR and thus determining the sum of the helical and non-helical components of the primordial magnetic field. The power spectrum of B-type polarization fluctuations, on the other hand, are sensitive only to the non-helical component of the primordial magnetic field. The primordial magnetic helicity can then be derived by combining these two sets of observations.

PACS numbers: 98.80.Cq

The cosmic microwave background radiation (CMBR) has become a remarkable tool for mapping the past and present states of the universe. As more refined observations are made, a larger array of theoretical ideas will be put to the test and more details of the history of the universe will emerge.

Until now, only the temperature anisotropy of the CMBR has been measured. It is widely recognized that even the most precise measurement of the temperature spectrum would still be compatible with a large class of initial conditions for the fluctuations in the primordial universe. Measurements of the CMBR polarization would significantly reduce this degeneracy. The much anticipated first detection of the CMBR polarization could be provided by the MAP satellite, launched by NASA in June of 2001, or balloon-borne B2K and MAX-IPOLE experiments. There are several other ongoing or planned ground-based experiments that have the detection of CMB polarization as their primary goal. However, most expectations of obtaining polarization spectra are connected with the Planck satellite mission, currently scheduled to be launched in 2007.

A possibility that has already received some attention is that large-scale Parity (P) violation may be observed via the CMBR [1, 2]. In Ref. [1] it was shown that a coherent magnetic field would induce non-zero P-violating correlations in the CMBR through Faraday rotation. In Ref. [2] the P violation was due to the dynamics of a pseu-

doscalar field which could induce a fixed-handed rotation of the polarization plane of the CMBR. In another case studied in Ref. [2], the pseudoscalar field could produce an excess of left- over right-handed polarization states of gravitational waves, which would be manifested in the CMBR as a P-violating signature. In Sec. I we examine the consequence of yet another possible source of P-violation (and also CP-violation), namely large-scale helical velocity flows (*i.e.* kinetic helicity) at recombination. We find that the CMBR temperature and polarization cross-correlators can provide a measurement of kinetic helicity (Sec. II). A motivation for considering helical flows is that helical magnetic fields may have been generated in the early universe [3, 4, 5, 6] and our initial guess was that such fields could induce helical velocities. However, in Sec. III we show that the magnitude of the kinetic helicity induced by helical magnetic fields is insignificant and does not lead to any observable signature in the CMBR.

This leaves us with the challenge of devising a methodology to observe the helicity of primordial magnetic fields. In Sec. IV we describe a method which involves observing the temperature and polarization fluctuations of the CMBR and also the Faraday rotation measure of the CMBR polarization along different directions. From a suitable combination of these observations, it is possible to extract the primordial magnetic field helicity. Hence, at least in principle, the helicity of cosmic magnetic fields

may be observable.

## I. KINETIC HELICITY

Kinetic helicity of a velocity field  $\mathbf{v}$  is characterized by a non-vanishing value of  $\langle \mathbf{v} \cdot \boldsymbol{\omega} \rangle$ , where  $\boldsymbol{\omega} \equiv \nabla \times \mathbf{v}$ . For the purpose of calculating the effect of helical flows on the cosmic microwave background radiation, it is useful to decompose the velocity field at last scattering into gradient components  $v^{(0)}$  and rotational components  $v^{(\pm 1)}$  as follows:

$$v_j(\mathbf{x}) = \int \frac{d^3k}{(2\pi)^3} e^{-i\mathbf{k}\cdot\mathbf{x}} \times \left( i\hat{k}_j v^{(0)} + Q_j^{(1)} v^{(1)} + Q_j^{(-1)} v^{(-1)} \right), \quad (1)$$

where

$$\mathbf{Q}^{(\pm 1)}(\mathbf{k}) \equiv -i \frac{\hat{\mathbf{e}}_1 \pm i\hat{\mathbf{e}}_2}{\sqrt{2}} \quad (2)$$

and the vectors  $\hat{\mathbf{e}}_{1,2}$  are such functions of  $\mathbf{k}$  that they form an orthonormal basis together with  $\hat{\mathbf{e}}_3 \equiv \hat{\mathbf{k}}$ . The functions  $\mathbf{Q}^{(\pm 1)}$  can be thought of as eigenvectors of helicity because  $i\hat{\mathbf{k}} \times \mathbf{Q}^{(s)} = s\mathbf{Q}^{(s)}$ , where  $s = \pm 1$ . Also,  $\mathbf{k} \cdot \mathbf{Q}^{(s)} = 0$  and  $\mathbf{Q}^{(s)}(\mathbf{k}) = \mathbf{Q}^{(-s)}(-\mathbf{k})$ . Under a parity transformation,  $\mathbf{v}(\mathbf{x}) \rightarrow -\mathbf{v}(-\mathbf{x})$ ,  $\mathbf{k} \rightarrow -\mathbf{k}$  while  $\mathbf{Q}^{(\pm 1)} \rightarrow \mathbf{Q}^{(\mp 1)}$  and therefore  $v^{(0)}(\mathbf{k}) \rightarrow -v^{(0)}(-\mathbf{k})$ ,  $v^{(\pm 1)}(\mathbf{k}) \rightarrow -v^{(\mp 1)}(-\mathbf{k})$ .

In Appendix A we will show that the parity-odd CMB correlators  $C_l^{TB}$  and  $C_l^{EB}$  are linearly dependent on the expectation value of the parity-odd combination of  $v^{(\pm 1)}$ :

$$\langle v^{(1)}(\mathbf{k}) v^{(1)}(-\mathbf{k}) - v^{(-1)}(\mathbf{k}) v^{(-1)}(-\mathbf{k}) \rangle. \quad (3)$$

The average helicity of the velocity field is proportional to the same quadratic combination of  $v^{(\pm 1)}$ . Namely,

$$\int d^3\mathbf{x} \mathbf{v}(\mathbf{x} + \mathbf{y}) \cdot [\nabla \times \mathbf{v}(\mathbf{x})] = \int \frac{d^3\mathbf{k}}{(2\pi)^3} k e^{i\mathbf{k}\cdot\mathbf{y}} \times \left( v^{(1)}(\mathbf{k}) v^{(1)}(-\mathbf{k}) - v^{(-1)}(\mathbf{k}) v^{(-1)}(-\mathbf{k}) \right), \quad (4)$$

where  $k \equiv |\mathbf{k}|$ .

Let us assume that the initial velocity field is random with a given power spectrum, such as

$$\langle v_i(\mathbf{k}) v_j(\mathbf{k}') \rangle = v_0^2 \frac{k^n}{k_*^{n+3}} (2\pi)^3 \delta(\mathbf{k} + \mathbf{k}') P_{ij}(\hat{\mathbf{k}}), \quad (5)$$

where  $v_0$  is the characteristic velocity of the flow and  $k_*$  is the wave vector corresponding to a cutoff scale. In general,  $P_{ij}$  does not have to be a symmetric tensor. The restrictions on it are: the reality condition  $P_{ij}^*(\hat{\mathbf{k}}) = P_{ij}(-\hat{\mathbf{k}}) = P_{ji}(\hat{\mathbf{k}})$ , the divergence-less condition (incompressibility)  $k^i P_{ij} = 0$ , and the requirement of correct transformation under rotations, which forces

$P_{ij}(\hat{\mathbf{k}})$  to be a tensorial function of  $\hat{k}^i$ . The latter condition is needed to ensure that the correlator  $P_{ij}(\hat{\mathbf{k}})$  describes a homogeneous and isotropic random vector field. It follows from these restrictions that

$$P_{ij}(\hat{\mathbf{k}}) = f(k) \left[ \delta_{ij} - \hat{k}_i \hat{k}_j \right] + ig(k) \varepsilon_{ijl} \hat{k}^l, \quad (6)$$

where  $f(k)$  and  $g(k)$  are real functions of  $k = |\mathbf{k}|$ . By using

$$\langle |\boldsymbol{\omega}(\mathbf{k}) \pm k\mathbf{v}(\mathbf{k})|^2 \rangle \geq 0,$$

where  $\boldsymbol{\omega}(\mathbf{k})$  is the Fourier transform of  $\boldsymbol{\omega}(\mathbf{x})$ , we can deduce that the functions  $f$  and  $g$  are not completely independent but must satisfy the inequality

$$f(\mathbf{k}) \geq |g(\mathbf{k})|. \quad (7)$$

[ $f(\mathbf{k}) \geq 0$  follows by taking the trace of Eq. (5).] Eqs. (1) and (5) now lead to

$$\begin{aligned} & \left\langle v^{(1)}(\mathbf{k}) v^{(1)}(\mathbf{k}') - v^{(-1)}(\mathbf{k}) v^{(-1)}(\mathbf{k}') \right\rangle \\ &= v_0^2 \frac{k^n}{k_*^{n+3}} (2\pi)^3 \delta(\mathbf{k} + \mathbf{k}') P^{ij}(\hat{\mathbf{k}}) Q_{[i}^{(1)}(\hat{\mathbf{k}}) Q_{j]}^{(-1)}(\hat{\mathbf{k}}). \end{aligned} \quad (8)$$

The  $f$ -term in Eq. (6) will not produce helicity because it is symmetric in  $i, j$ . Since

$$i\varepsilon_{ijl} \hat{k}^l Q_{[i}^{(1)}(\hat{\mathbf{k}}) Q_{j]}^{(-1)}(\hat{\mathbf{k}}) = 1, \quad (9)$$

we get

$$\begin{aligned} & \left\langle v^{(1)}(\mathbf{k}) v^{(1)}(\mathbf{k}') - v^{(-1)}(\mathbf{k}) v^{(-1)}(\mathbf{k}') \right\rangle \\ &= v_0^2 \frac{k^n}{k_*^{n+3}} (2\pi)^3 \delta(\mathbf{k} + \mathbf{k}') g(k). \end{aligned} \quad (10)$$

## II. CMBR SIGNATURE OF KINETIC HELICITY

The CMBR temperature and polarization at a given direction on the sky are described by time-averaged components of the electric field intensity tensor  $I_{ij} \equiv E_i E_j$ . Equivalently, the CMBR is represented by the Stokes parameters  $I, Q, U$  and  $V$  [7, 8], where  $I$  is the total intensity,  $Q$  and  $U$  are two components of the linear polarization and  $V$  quantifies the circular polarization. Assuming that the CMB photons prior to the last scattering were unpolarized, we can drop  $V$  from consideration, since Thomson scattering can only generate linear polarization.

Decomposing the temperature anisotropy into spherical harmonics gives

$$\Delta(\hat{\mathbf{n}}) \equiv \frac{T(\hat{\mathbf{n}}) - \bar{T}}{\bar{T}} = \sum_{l,m} Y_{lm}(\hat{\mathbf{n}}) a_{lm}^T. \quad (11)$$

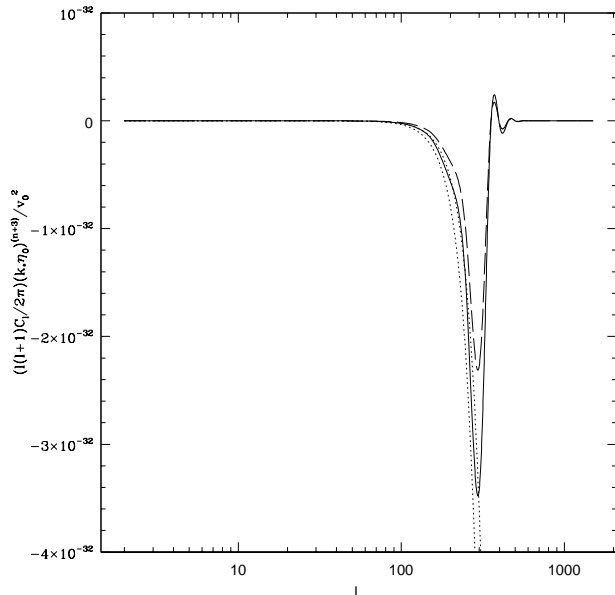


FIG. 1:  $(1/2\pi)l(l+1)C_l^{TB,EB}(k_*\eta_0)^{n+3}/v_0^2$  vs  $l$  for  $n = 2$  and  $2\pi/k_* = 288$  Mpc, where  $n$ ,  $k_*$  and  $v_0$  are defined in Eq. (5) and  $\eta_0$  is the conformal time today. We have also taken  $g(k) = 1$  [defined in Eq. (6)]. The solid line shows the  $TB$  correlation and the dashed line is  $EB$ . Dotted lines show the same spectra in the absence of a cutoff.

Analogously,  $Q(\hat{\mathbf{n}})$  and  $U(\hat{\mathbf{n}})$  can be decomposed using spin-2 spherical harmonics (see Refs. [1, 9]):

$$(Q \pm iU)(\hat{\mathbf{n}}) = \sum_{l,m} \pm_2 Y_{lm} a_{lm}^{(\pm 2)}. \quad (12)$$

The “electric” and “magnetic” components of polarization are eigenstates of parity and may be defined by

$$a_{lm}^E = -\frac{1}{2} (a_{lm}^{(2)} + a_{lm}^{(-2)}), \quad a_{lm}^B = -\frac{1}{2i} (a_{lm}^{(2)} - a_{lm}^{(-2)}). \quad (13)$$

Under parity inversion the components transform as  $a_{lm}^{T,E} \rightarrow (-1)^l a_{lm}^{T,E}$ , while  $a_{lm}^B \rightarrow -(-1)^l a_{lm}^B$ .

Observations of CMBR are usually presented in the form of spectral functions  $C_l^{X,Y}$  defined by

$$C_l^{XY} = \frac{1}{2l+1} \sum_{m=-l}^l \langle (a_{lm}^X)^* a_{lm}^Y \rangle, \quad (14)$$

where  $X$  and  $Y$  stand for  $T$ ,  $E$  or  $B$ . Correlators in Eq. (14) are real because they involve summation over both positive and negative values of  $m$ . This can be seen by noting that the tensor spherical harmonics  ${}_s Y_{lm}$  satisfy

$$[{}_s Y_{lm}]^* = (-1)^{s+m} {}_{-s} Y_{l,-m}, \quad (15)$$

and therefore the components  $a_{lm}^{\pm 2}$ ,  $a_{lm}^{T,E,B}$  transform un-

der complex conjugation as

$$[a_{lm}^{\pm 2}]^* = (-1)^m a_{l,-m}^{\mp 2}, \quad [a_{lm}^{T,E,B}]^* = (-1)^m a_{l,-m}^{T,E,B}. \quad (16)$$

The correlators  $C_l^{TB}$  and  $C_l^{EB}$  are parity-odd, while all other correlators  $C_l^{XY}$  are parity-even. If no parity-odd sources are present, the ensemble of fluctuations is statistically parity-symmetric and therefore the correlators  $C_l^{TB}$  and  $C_l^{EB}$  must vanish. This is the case in most of the literature on CMBR polarization. In our case, however, the presence of parity-violating sources allows nonzero values of the parity-odd correlators  $C_l^{TB}$  and  $C_l^{EB}$  and hence these correlators are of special interest to us.

The details of the calculation of  $C_l^{TB}$  and  $C_l^{EB}$  are given in Appendix A, where we find some limiting forms of these functions. We have performed numerical evaluations for several different values of  $n$  and  $k_*$  [defined in Eq. (5)] and assuming  $g(k) = 1$  [defined in Eq. (6)]. The results for  $n = 2$ ,  $n = -2$  and  $n = -3$  are shown in Figs. 1-3. The cosmological parameters were set to  $\Omega_\Lambda = 0.7$ ,  $\Omega_{\text{CDM}} = 0.25$ ,  $\Omega_{\text{Baryons}} = 0.05$  and  $h = 65$  km sec $^{-1}$  Mpc $^{-1}$ . With this choice of parameters, the conformal time today is  $\eta_0 \approx 1.5 \times 10^4$  Mpc (we use units in which the speed of light and the scale factor at present time are set to 1).

For  $n \geq -1$ , the angular power spectra of  $TB$  and  $EB$  correlations are dominated by the cutoff. In Fig. 1, for which we have taken  $n = 2$ , the position of the main peak in the plots of  $(1/2\pi)l(l+1)C_l^{TB}$  and  $(1/2\pi)l(l+1)C_l^{EB}$  vs  $l$  corresponds to the cutoff value of  $2\pi/k_* = 288$  Mpc or  $k_*\eta_0 \approx 330$ . The dotted lines illustrate that spectra diverge at large  $l$  in the absence of the cutoff.

As the value of  $n$  is decreased, the correlations gradually become cutoff-independent. In Fig. 2 we plot the spectra for  $n = -2$  with a cutoff at  $2\pi/k_* = 288$  Mpc and without a cutoff. As can be seen from the plot, above a certain scale ( $l \lesssim 300$ ) the spectra do not depend on the cutoff and exhibit a potentially interesting peak structure. However, spectra still diverge on smaller scales in the absence of a cutoff.

Clearly, any constraint imposed by the future data on  $v_0$  and  $k_*$  will be  $n$ -dependent. In particular, with the chosen form of the initial power spectrum [Eq. (10)], for  $n \geq -2$  a measurement of  $C_l^{TB}$  or  $C_l^{EB}$  would not constrain the helical flow at all. For example, if we optimistically assume that  $(1/2\pi)l(l+1)C_l^{TB} \sim 10^{-10}$ , then for  $n = 2$  and  $2\pi/k_* = 288$  Mpc we obtain that  $v_0 \lesssim 10^{17}$ , which is not a very useful bound. For  $n = -3$  and  $n = -4$ , with the same value of  $2\pi/k_*$ , we find  $v_0 \lesssim 10^{-5}$  and  $v_0 \lesssim 10^{-11}$  respectively.

Causality will, in general, constrain the value of the spectral index  $n$  from below. The bound is obtained by setting the real space velocity correlation function to zero at causally prohibited separations. This constrains the Fourier transform of the correlator to be an analytical function of  $k$ , which, in turn, implies that  $n \geq 2$  for small  $k$ . Thus, our analysis suggests that the CMBR will

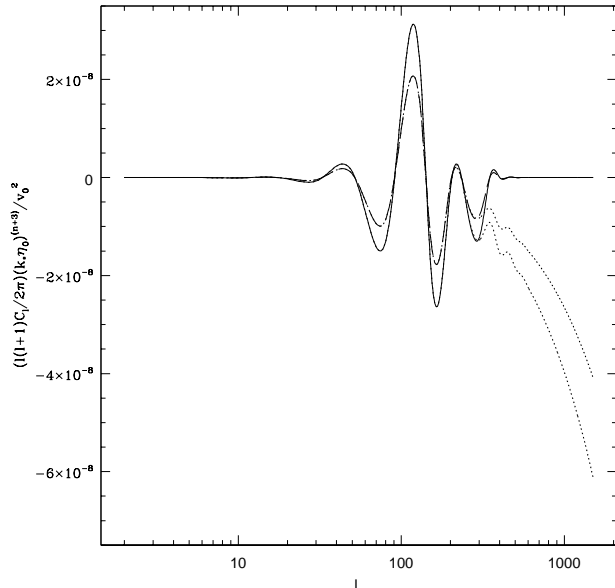


FIG. 2: Same spectra as in Fig. 1 for  $n = -2$  with (solid and dashed lines) and without (dotted lines) presence of a cutoff at  $2\pi/k_* = 288$  Mpc.

not be able to constrain primordial kinetic helicity unless acausal physics is responsible for producing them. Since models that best fit the CMBR temperature power spectrum do rely on causality being violated in the past, by *e.g.* inflation or a larger speed of light, it is not inconceivable that the velocity correlations would be acausal as well.

### III. KINETIC HELICITY FROM MAGNETIC HELICITY?

In this section we explore the possibility that helical magnetic fields may induce kinetic helicity  $\omega$  at last scattering. As we shall see, the induced velocities are insignificant and can be ignored.

We shall be interested in the effects of a statistically homogeneous and isotropic magnetic field, with possibly non-vanishing helicity. If we denote the Fourier amplitudes of the magnetic field by  $\mathbf{b}(\mathbf{k})$ , then, as in Sec. I,

$$\langle b_i(\mathbf{k})b_j(\mathbf{k}') \rangle = (2\pi)^3 \delta^{(3)}(\mathbf{k} + \mathbf{k}') \times [(\delta_{ij} - \hat{k}_i \hat{k}_j)S(k) + i\varepsilon_{ijl} \hat{k}_l A(k)]. \quad (17)$$

Here  $S(k)$  denotes the symmetric part and  $A(k)$  the antisymmetric part of the correlator. These functions are constrained by [10]

$$S(\mathbf{k}) \geq |A(\mathbf{k})| \quad (18)$$

and  $S(\mathbf{k}) \geq 0$ , exactly as in the case of kinetic helicity [Eq. (7)]. Furthermore,

$$\langle \mathbf{B}(\mathbf{x}) \cdot [\nabla \times \mathbf{B}(\mathbf{x})] \rangle$$

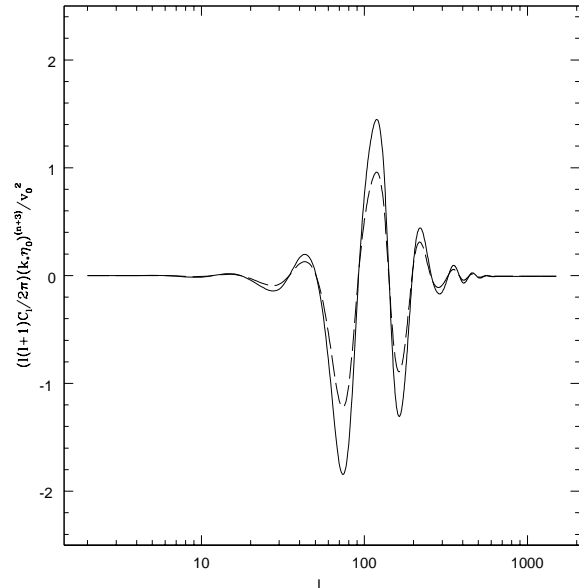


FIG. 3: Same spectra as in Fig. 1 for  $n = -3$ . Spectra no longer depend on the cutoff scale.

only depends on  $A(k)$  and not on  $S(k)$ . Therefore  $A(k)$  represents the helical component of the magnetic field and  $S(k)$  the non-helical component.

The Lorentz force  $\mathbf{F}_L$  due to the magnetic field on the (electrically neutral) cosmic plasma is

$$\mathbf{F}_L = \mathbf{j} \times \mathbf{B}, \quad (19)$$

where  $\mathbf{j}$  is the electric current that satisfies Maxwell's equation in the MHD approximation:

$$\mathbf{j} = \nabla \times \mathbf{B}. \quad (20)$$

Therefore

$$\langle \mathbf{F}_L \rangle = \langle \mathbf{B}(\mathbf{x}) \times [\nabla \times \mathbf{B}(\mathbf{x})] \rangle. \quad (21)$$

In the tight-coupling approximation, in which it is assumed that velocities of photons, electrons and protons are approximately the same, the Lorentz force induces flows of neutral plasma.<sup>1</sup> An evaluation shows that the quantity  $\langle \mathbf{F}_L \rangle$  depends on  $S(k)$  but has no dependence on  $A(k)$ . In other words, the term with  $A(k)$  denotes the “force-free” component of the magnetic field. Therefore the velocity flow at last scattering is unaffected by the

<sup>1</sup> In the tight-coupling approximation the photons, electrons and protons are treated as a single fluid. However, the current  $\mathbf{j}$  is proportional to the difference in velocities of electron and proton fluids. It is the Lorentz force due to this slight difference in velocities that drives flows in neutral plasma.

helical component and the corresponding Doppler signature on the CMBR can only carry information about  $S(k)$  and no information about  $A(k)$ .

In the preceding discussion, based on the tight-coupling approximation, we assumed that the Lorentz force acts on an element of the neutral plasma and changes its velocity. In reality the coupling of photons to electrons is much stronger than that to protons and so the plasma at recombination is better treated as composed of two fluids, namely the electron-photon fluid and the proton fluid. It is precisely in this approximation that the generation of magnetic fields due to cosmic vorticity was analyzed by Harrison [11].

Our situation is similar to Harrison's, except for initial conditions: we have an initial (force-free) helical magnetic field and we need to find the velocity induced by it. The analysis, described in Appendix B, closely follows that of Harrison. The result is that the electron-photon fluid will gain a vorticity  $\omega_e$  given by

$$\omega_e = \frac{1}{en_e} \nabla^2 \mathbf{B}, \quad (22)$$

where  $e$  is the electron charge and  $n_e$  is the electron number density. If we estimate  $|\nabla^2 \mathbf{B}| \sim B/L^2$ , where  $L$  is the coherence scale of the field, we find

$$|\mathbf{v}| \sim |L\omega_e| \sim 10^{-18} \left( \frac{B_0}{10^{-9}\text{G}} \right) \left( \frac{1\text{kpc}}{L_0} \right), \quad (23)$$

where  $B_0$  and  $L_0$  denote the magnetic field strength and coherence scale at the present epoch and the cosmic electron number density is  $\sim 10^{-6}/\text{cm}^3$ . (Current bounds on cosmic magnetic fields constrain the field strength to be less than  $\sim 10^{-9}$  G.) Compared to the velocities induced by gravitational perturbations ( $\sim 10^{-5}$ ) the velocities induced by helical fields are insignificant.

#### IV. A STRATEGY TO DETECT MAGNETIC HELICITY

In the previous section we have shown that only the non-helical component of the magnetic field can have a signature in the Doppler contribution to the CMBR. If we could find another observable that is sensitive to both the non-helical and the helical components, we could combine observations and extract the helical component of the magnetic field. An observable that does depend on both helical and non-helical components is the Faraday rotation of linearly polarized sources due to light propagation through a magnetized plasma.

The CMBR is expected to be linearly polarized and so any intervening magnetic fields will rotate the polarization vector at a rate given by:

$$d\theta = \lambda^2 \frac{e^3}{8\pi^2 m_e^2} a n_e \mathbf{B} \cdot d\mathbf{l}, \quad (24)$$

where  $\lambda$  is the wavelength of light,  $a$  is the scale factor normalized so that  $a_{\text{today}} = 1$ ,  $n_e$  is the number density of free electrons,  $d\mathbf{l}$  is the comoving length element along the photon trajectory from the source to the observer and we are using natural units with  $\hbar = c = 1$  and  $\alpha = e^2/(4\pi) \approx 1/137$ . Using the known expression for Thomson scattering cross-section,

$$\sigma_T = \frac{8\pi\alpha^2}{3m_e^2}, \quad (25)$$

and integrating along the line of sight, we obtain from Eq. (24):

$$\theta = \frac{3}{2\pi e} \lambda_0^2 \int \dot{\tau}(\mathbf{x}) \tilde{\mathbf{B}} \cdot d\mathbf{l} \quad (26)$$

where  $\dot{\tau}(\mathbf{x}) \equiv n_e \sigma_T a$  is the differential optical depth along the line of sight,  $\lambda_0$  is the observed wavelength of the radiation and  $\tilde{\mathbf{B}} \equiv \mathbf{B}a^2$  is the ‘‘comoving’’ magnetic field.

Faraday rotation depends on the free electron density, which becomes negligible towards the end of recombination. Therefore, the bulk of the rotation is produced during a relatively brief period of time when the electron density is sufficiently low for polarization to be produced and yet sufficiently high for the Faraday rotation to occur. The average Faraday rotation (in radians) between Thomson scatterings due to a tangled magnetic field was calculated in Ref. [12] and is given by

$$F = \frac{3}{2\pi e} \frac{B_0}{\nu_0^2} \approx 0.08 \left( \frac{B_0}{10^{-9}\text{G}} \right) \left( \frac{30\text{GHz}}{\nu_0} \right)^2, \quad (27)$$

where  $B_0$  is the current amplitude of the field and  $\nu_0$  is the radiation frequency observed today.

The amplitude of the CMB polarization fluctuations is expected to be of order  $10^{-6}$ , an order of magnitude lower than that of the temperature fluctuations. As discussed in Ref. [13], detecting a Faraday rotation of order  $1^\circ$  will require a measurement which is superior in sensitivity by another factor of  $10^2$ . Such accuracy is at the limit of current experimental proposals but there is a hope that it will eventually be accomplished.

It is usual to define the wavelength independent ‘‘rotation measure’’ (RM) as:

$$\text{RM} = \frac{3}{2\pi e} \int \dot{\tau}(\mathbf{x}) \tilde{\mathbf{B}} \cdot d\mathbf{l} \quad (28)$$

A polarization map of the CMBR at several wavelengths will (in principle) give  $\theta$  as a function of  $\lambda$  along different directions in the sky. From this information the rotation measure in any given direction in the sky can be determined. Hence the polarization map of the CMBR will also lead to a ‘‘rotation measure map’’. Then we can find correlations of the RM:

$$RR' \equiv \langle \text{RM}(\hat{\mathbf{n}}) \text{RM}(\hat{\mathbf{n}}') \rangle, \quad (29)$$

where  $\text{RM}(\hat{\mathbf{n}})$  is the rotation measure of the CMBR, observed along the direction  $\hat{\mathbf{n}}$ . Using Eq. (17), this yields

$$RR' = \left(\frac{3}{2\pi e}\right)^2 \int \frac{d^3k}{(2\pi)^3} [\alpha S(k) + \beta A(k)], \quad (30)$$

where

$$\alpha \equiv \mathbf{K}_1 \cdot \mathbf{K}_2^* - (\hat{\mathbf{k}} \cdot \mathbf{K}_1)(\hat{\mathbf{k}} \cdot \mathbf{K}_2^*), \quad (31)$$

$$\beta \equiv i\hat{\mathbf{k}} \cdot (\mathbf{K}_1 \times \mathbf{K}_2^*), \quad (32)$$

$$\mathbf{K}_1 \equiv \hat{\mathbf{n}} \int d\eta \dot{\tau}(\eta) e^{-i\hat{\mathbf{k}} \cdot \hat{\mathbf{n}}\eta}, \quad (33)$$

$$\mathbf{K}_2^* \equiv \hat{\mathbf{n}}' \int d\eta \dot{\tau}(\eta) e^{+i\hat{\mathbf{k}} \cdot \hat{\mathbf{n}}'\eta}. \quad (34)$$

Eqs. (33) and (34) are obtained under the assumption that effects of inhomogeneities in free electron density along different directions on the sky are of the next order in perturbation theory. That allows us to write  $\dot{\tau}(\mathbf{x}) = \dot{\tau}(\eta)$  and  $d\mathbf{l} = \hat{\mathbf{n}}d\eta$ .

A crucial feature of  $RR'$  is that it depends on both the helical and non-helical spectral functions  $S(k)$  and  $A(k)$ .

The CMBR polarization spectra induced by tangled magnetic fields have already been calculated by Seshadri and Subramanian [14]. They computed the correlator between the B-type polarization of the CMBR photons commonly denoted by  $C_l^{BB}$ . Defining

$$\Delta T^{BB}(l) = T_0 \sqrt{\frac{l(l+1)}{2\pi}} C_l^{BB},$$

where  $T_0$  is the CMBR temperature, they found (Eq. (8) in Ref. [14]) that for  $l > 1500$ ,

$$\Delta T^{BB}(l) \simeq (0.93\mu\text{K}) I \left(\frac{l}{R_*}\right) \left[\frac{B_{\text{rms}}}{3.10^{-9}\text{G}}\right]^2 \left[\frac{l}{1500}\right]^{-1/2}. \quad (35)$$

Here  $B_{\text{rms}}$  is the rms magnetic field strength at the present epoch and  $R_* \equiv \eta_0 - \eta_*$  is the conformal time interval from last scattering to the present epoch. The spectral functions  $S(k)$  are contained in the mode-coupling integral  $I(l/R_*)$  as follows:

$$I^2(k) = \int_0^\infty \frac{dq}{q} \int_{-1}^{+1} d\mu \frac{h(q)h(|\mathbf{k} + \mathbf{q}|)k^3}{|\mathbf{k} + \mathbf{q}|^3} \times (1 - \mu^2) \left[1 + \frac{(k + 2q\mu)(k + q\mu)}{|\mathbf{k} + \mathbf{q}|^2}\right], \quad (36)$$

where  $|\mathbf{k} + \mathbf{q}| = (k^2 + q^2 + 2kq\mu)^{1/2}$  and

$$h(k) \equiv \frac{k^3 S(k)}{\pi^2 B_{\text{rms}}^2}. \quad (37)$$

The exact form of the Seshadri and Subramanian's result is not important for describing our strategy to isolate the helical component of the magnetic field. We need only observe the crucial feature that  $\Delta T^{BB}(l)$ , and hence  $C_l^{BB}$ , depends on the non-helical spectral function  $S(k)$  and is independent of the helical spectral function  $A(k)$ . This is because, as discussed in the previous section,  $A(k)$  is the force-free component of the magnetic field and does not induce any velocity in the last scattering surface. However, it is worth noting a few assumptions that enter the analysis in Ref. [14]. The first is an assumption of Gaussianity by which 4-point functions of the magnetic field can be factored into a product of 2 point functions. The second is the assumption that the effects of Faraday rotation at last scattering are not important. The latter assumption is justified at the high frequencies of observation planned for the Planck satellite [14].

Hence, if we could use  $C_l^{BB}$  to obtain  $S(k)$  – which would only be possible assuming some functional form (such as a power law) for  $S(k)$  since  $S(k)$  occurs within some integrals in Eq. (36) – we could insert the result in the expression for  $RR'$  given in Eq. (30). This will isolate  $A(k)$  in Eq. (30) and, with some assumptions about the functional form of  $A(k)$ , the cosmic magnetic helicity can be evaluated. Even if the assumptions in the derivation of Eq. (35) are not completely valid, the RM correlator in Eq. (30) and  $C_l^{BB}$  have different dependencies on  $S(k)$  and  $A(k)$ , and hence the two observations can be used to disentangle these two spectral functions.

## V. CONCLUSIONS

We have analyzed certain P- and CP-violating signatures in the CMBR. If there is kinetic helicity at last scattering, it would imprint a signature in the cross-correlators  $C_l^{TB}$  and  $C_l^{EB}$ . Kinetic helicity can be induced by helical magnetic fields but the effect is too small to be significant since the helical component of magnetic fields is force-free. Instead we have proposed another strategy for detecting the helicity of primordial magnetic fields using polarization and rotation measure maps of the CMBR.

The helical magnetic fields produced during electroweak baryogenesis ( $\sim 10^{-13}$  G at last scattering) are several orders weaker than current upper bounds on the magnetic field strength ( $\sim 10^{-6}$  G) at last scattering [5]. Therefore the detection of electroweak fields does not seem feasible with forthcoming experiments. However, it is conceivable that stronger helical fields were produced due to some other mechanism and so it is still important to think of strategies for detecting primordial magnetic fields and helicity.

### Acknowledgments

TV is grateful to George Field and Kandu Subramanian for discussions. LP acknowledges helpful conversations with Luis Mendes. This work was supported by DoE grant number DEFG0295ER40898 at CWRU. LP is supported by PPARC. SW is supported by the NSF. LP and TV would like to thank the organizers of the July 2001 ESF COSLAB Programme workshop at Imperial College, London, during which this project was started.

### APPENDIX A

Here we outline our calculation of the signature of kinetic helicity in the CMBR.

In the ‘‘total angular momentum’’ formalism of Hu and White [9], the observable CMB anisotropies  $T, Q$ , and  $U$  are expanded into a set of components  $\Theta_l^{(m)}, E_l^{(m)}, B_l^{(m)}$ , which are functions of  $k$  and  $\eta$ ; here  $k$  is the wavenumber in Fourier space and  $\eta$  is the conformal time. These quantities are such that the power spectra  $C_l^{XY}$  are expressed through the  $l$ -th components only (see Eq. (56) of [9]), *e.g.*

$$C_l^{TB} = \frac{2}{\pi} \int dk k^2 \sum_{m=-2}^2 \frac{[\Theta_l^{(m)}(k, \eta_0)]^*}{2l+1} \frac{B_l^{(m)}(k, \eta_0)}{2l+1}, \quad (\text{A1})$$

$$C_l^{EB} = \frac{2}{\pi} \int dk k^2 \sum_{m=-2}^2 \frac{[E_l^{(m)}(k, \eta_0)]^*}{2l+1} \frac{B_l^{(m)}(k, \eta_0)}{2l+1}, \quad (\text{A2})$$

where  $m = 0, m = \pm 1$  and  $m = \pm 2$  denote scalar, vector and tensor contributions respectively, and  $\eta_0$  is the conformal time today. The quantities  $\Theta_l^{(m)}, E_l^{(m)}, B_l^{(m)}$ , in turn, are found from the linearized Einstein and Boltzmann equations and are expressed as integrals along the line-of-sight of primordial perturbation sources (initial density and velocity perturbations). Assuming that the perturbation sources are random fields with known correlations in Fourier space, one can find the expectation value of any quadratic combination of  $T, Q$  and  $U$  or, equivalently, power spectra  $C_l^{TT, EE, BB}$  and cross-correlators  $C_l^{TE, TB, EB}$ .

Scalar perturbations do not generate  $B$ -type polarization. We will also assume that there are no parity violating tensor sources. The integral solution of the Boltzmann equations for the components  $\Theta_l^{(\pm 1)}, E_l^{(\pm 1)}, B_l^{(\pm 1)}$  is given by Eqs. (79) and (77) of Ref. [9],

$$\begin{aligned} & \frac{\Theta_l^{(\pm 1)}(\eta_0, k)}{2l+1} \\ &= \int_0^{\eta_0} d\eta e^{-\tau} \left[ \dot{\tau} (v^{(\pm 1)} - V) j_l^{1, \pm 1}(k(\eta_0 - \eta)) \right. \end{aligned}$$

$$\left. + (\dot{\tau} P^{(\pm 1)} + \frac{kV}{\sqrt{3}}) j_l^{2, \pm 1}(k(\eta_0 - \eta)) \right], \quad (\text{A3})$$

$$\begin{aligned} \frac{E_l^{(\pm 1)}(\eta_0, k)}{2l+1} &= -\sqrt{6} \int_0^{\eta_0} d\eta \dot{\tau} e^{-\tau} \\ &\times P^{(\pm 1)}(k, \eta) \varepsilon_l^{(\pm 1)}(k(\eta_0 - \eta)), \quad (\text{A4}) \end{aligned}$$

$$\begin{aligned} \frac{B_l^{(\pm 1)}(\eta_0, k)}{2l+1} &= -\sqrt{6} \int_0^{\eta_0} d\eta \dot{\tau} e^{-\tau} \\ &\times P^{(\pm 1)}(k, \eta) \beta_l^{(\pm 1)}(k(\eta_0 - \eta)), \quad (\text{A5}) \end{aligned}$$

where  $V$  is the vector component of the metric perturbations,  $\dot{\tau}$  is the differential optical depth,  $\tau(\eta) = \int_\eta^{\eta_0} \dot{\tau}(\eta') d\eta'$ , and

$$P^{(\pm 1)}(k, \eta) \equiv \frac{1}{10} \left( \Theta_2^{(\pm 1)} - \sqrt{6} E_2^{(\pm 1)} \right). \quad (\text{A6})$$

The functions  $j_l^{1, \pm 1}, j_l^{2, \pm 1}, \varepsilon_l^{(\pm 1)}$  and  $\beta_l^{(\pm 1)}$  satisfy  $j_l^{11} = j_l^{1, -1}, j_l^{21} = j_l^{2, -1}, \varepsilon_l^{(1)} = \varepsilon_l^{(-1)}$  and  $\beta_l^{(1)} = -\beta_l^{(-1)}$ , where

$$j_l^{11}(x) \equiv \sqrt{\frac{l(l+1)}{2}} \frac{j_l(x)}{x}, \quad (\text{A7})$$

$$j_l^{21}(x) \equiv \sqrt{\frac{3l(l+1)}{2}} \frac{d}{dx} \left( \frac{j_l(x)}{x} \right), \quad (\text{A8})$$

$$\varepsilon_l^{(1)}(x) \equiv \frac{\sqrt{(l-1)(l+2)}}{2} \left( \frac{j_l'(x)}{x} + \frac{j_l(x)}{x^2} \right), \quad (\text{A9})$$

$$\beta_l^{(1)}(x) \equiv \frac{\sqrt{(l-1)(l+2)}}{2} \frac{j_l(x)}{x}, \quad (\text{A10})$$

and  $j_l(x)$  is the spherical Bessel function. It is easy to see that, for instance, the correlator  $C_l^{EB}$  depends on the parity-odd combination  $P^{(1)}P^{(1)} - P^{(-1)}P^{(-1)}$ .

The CMBR anisotropies sourced by velocity flows are predominantly due to the Doppler effect. Since the net effect is expected to be small, it is a good approximation to keep only terms that are of lowest non-trivial order in  $v^{(\pm 1)}$  and in the tight coupling approximation. Then Eq. (A3) becomes

$$\begin{aligned} \frac{\Theta_l^{(\pm 1)}(\eta_0, k)}{2l+1} &= \int_0^{\eta_0} d\eta \dot{\tau} e^{-\tau} \\ &\times v^{(\pm 1)}(k, \eta) j_l^{1, \pm 1}(k(\eta_0 - \eta)). \quad (\text{A11}) \end{aligned}$$

One can express functions  $P^{(\pm 1)}$  in terms of  $v^{(\pm 1)}$  using the linearized Boltzmann equations for temperature and polarization anisotropies written in form of infinite recursive series in multipole index  $l$  (see equations (60), (63) and (64) of [9]). The relevant equations are:

$$\dot{\Theta}_1^{(\pm 1)} = -k \frac{\sqrt{3}}{5} \Theta_2^{(\pm 1)} - \dot{\tau} (\Theta_1^{(\pm 1)} - v^{(\pm 1)} - \dot{V}), \quad (\text{A12})$$

$$\dot{\Theta}_2^{(\pm 1)} = k \left[ \frac{1}{\sqrt{3}} \Theta_1^{(\pm 1)} - \frac{2\sqrt{2}}{7} \Theta_3^{(\pm 1)} \right] - \dot{\tau} (\Theta_2^{(\pm 1)} - P^{(\pm 1)}), \quad (\text{A13})$$

$$\dot{E}_2^{(\pm 1)} = -k \frac{\sqrt{40}}{7\sqrt{9}} E_3^{(\pm 1)} - \dot{\tau} (E_2^{(\pm 1)} + \sqrt{6} P^{(\pm 1)}). \quad (\text{A14})$$

If vector metric perturbations are exclusively due to velocity flows, then  $\dot{V}$  is of second order in  $v^{\pm 1}$  and its effect on CMBR photons is small compared to the induced Doppler shifts. Tight coupling implies that the mean free path of photons is negligible compared to the scales under consideration:  $\dot{\tau}^{-1} \rightarrow 0$  and  $k/\dot{\tau} \ll 1$ . From Eq. (A12), to 0-th order in the tight coupling approximation, we obtain  $\Theta_1^{(\pm 1)} = v^{(\pm 1)}$ . To the same order, from Eqs. (A14) and (A6), we find that

$$E_2^{(\pm 1)} = -\frac{\sqrt{6}}{4} \Theta_2^{(\pm 1)}. \quad (\text{A15})$$

The quadrupole moments  $\Theta_2^{(\pm 1)}$  and  $P^{(\pm 1)}$  vanish when  $\dot{\tau}^{-1} \rightarrow 0$ . However, a non-zero dipole term generates the quadrupole moments in the next lowest order in  $k/\dot{\tau}$ . Using Eqs. (A6) and (A15), Eq. (A13) can be re-written as:

$$\Theta_2^{(\pm 1)} - \frac{4}{3} \dot{\tau}^{-1} \dot{\Theta}_2^{(\pm 1)} + \frac{4k}{3\dot{\tau}} \frac{2\sqrt{2}}{7} \Theta_3^{(\pm 1)} = \frac{4k}{3\sqrt{3}\dot{\tau}} \Theta_1^{(\pm 1)}. \quad (\text{A16})$$

In the above, the RHS is the source, namely, each of the terms on the LHS would be zero in the absence of  $\Theta_1^{(1)}$ . On the LHS, the leading order (in tight coupling) term is  $\Theta_2^{(\pm 1)}$ . Therefore,  $\Theta_2^{(\pm 1)} \approx 4kv^{(\pm 1)}/(3\sqrt{3}\dot{\tau})$  and

$$P^{(\pm 1)} \approx \frac{kv^{(\pm 1)}}{3\sqrt{3}\dot{\tau}}, \quad (\text{A17})$$

From Eqs. (A4), (A5), (A11) and (A17) we obtain the following expressions for the spectral correlators  $C_l^{TB}$  and  $C_l^{EB}$ :

$$C_l^{TB} = -\frac{2\sqrt{2}}{3\pi} \int_0^\infty k^2 dk k \int_0^{\eta_0} d\eta_1 \int_0^{\eta_0} d\eta_2 \quad (\text{A18})$$

$$\times e^{-\tau(\eta_1)} e^{-\tau(\eta_2)} \varepsilon_l^{(1)}(k(\eta_0 - \eta_1)) j_l^{11}(k(\eta_0 - \eta_2))$$

$$\times \langle v^{(1)}(k, \eta_1) v^{(1)}(k, \eta_2) - v^{(-1)}(k, \eta_1) v^{(-1)}(k, \eta_2) \rangle.$$

$$C_l^{EB} = \frac{4}{9\pi} \int_0^\infty k^2 dk k^2 \int_0^{\eta_0} d\eta_1 \int_0^{\eta_0} d\eta_2 \quad (\text{A19})$$

$$\times e^{-\tau(\eta_1)} e^{-\tau(\eta_2)} \varepsilon_l^{(1)}(k(\eta_0 - \eta_1)) \beta_l^{(1)}(k(\eta_0 - \eta_2))$$

$$\times \langle v^{(1)}(k, \eta_1) v^{(1)}(k, \eta_2) - v^{(-1)}(k, \eta_1) v^{(-1)}(k, \eta_2) \rangle.$$

If we assume that the time-evolution of each Fourier mode of the velocity field is independent of  $k$ , *i.e.* the evolution equations contain only  $k = |\mathbf{k}|$ , then we can write the unequal time correlator in Eqs. (A18) and (A19) as a product of the initial power spectrum and the evolution functions  $\mathcal{T}(k, \eta)$ :

$$\langle v^{(1)}(k, \eta_1) v^{(1)}(k, \eta_2) - v^{(-1)}(k, \eta_1) v^{(-1)}(k, \eta_2) \rangle$$

$$= \mathcal{T}(k, \eta_1) \mathcal{T}(k, \eta_2)$$

$$\times \langle v^{(1)}(k) v^{(1)}(k) - v^{(-1)}(k) v^{(-1)}(k) \rangle, \quad (\text{A20})$$

where  $\langle v^{(1)}(k) v^{(1)}(k) - v^{(-1)}(k) v^{(-1)}(k) \rangle$  is the spectrum evaluated at some initial time which we choose to be the time of recombination. Using Eq. (10) for the velocity power spectrum together with Eqs. (A18-A20), we can write  $C_l^{TB}$  and  $C_l^{EB}$  as

$$C_l^{TB} = \frac{2}{\pi} \int_0^\infty k^2 dk v_0^2 \frac{k^n}{k_*^{n+3}} g(k) \tilde{\Delta}_l(k) \tilde{B}_l(k), \quad (\text{A21})$$

$$C_l^{EB} = \frac{2}{\pi} \int_0^\infty k^2 dk v_0^2 \frac{k^n}{k_*^{n+3}} g(k) \tilde{E}_l(k) \tilde{B}_l(k), \quad (\text{A22})$$

where

$$\tilde{\Delta}_l(k) \equiv \int_0^{\eta_0} d\eta e^{-\tau \dot{\tau}} j_l^{11}(k(\eta_0 - \eta)) \mathcal{T}(k, \eta)$$

$$= \sqrt{\frac{l(l+1)}{2}} \int_0^{\eta_0} d\eta \frac{j_l(k(\eta_0 - \eta))}{k(\eta_0 - \eta)}$$

$$\times \mathcal{T}(k, \eta) \dot{\tau} e^{-\tau}, \quad (\text{A23})$$

$$\tilde{E}_l(k) \equiv -\frac{\sqrt{2}}{3} \int_0^{\eta_0} d\eta e^{-\tau} \varepsilon_l^{(1)}(k(\eta_0 - \eta)) \mathcal{T}(k, \eta)$$

$$= -\frac{\sqrt{(l-1)(l+1)}}{3\sqrt{2}} \int_0^{\eta_0} d\eta \frac{j_l(k(\eta_0 - \eta))}{k(\eta_0 - \eta)}$$

$$\times \frac{\partial}{\partial \eta} (e^{-\tau} \mathcal{T}(k, \eta)), \quad (\text{A24})$$

$$\tilde{B}_l(k) \equiv -\frac{\sqrt{2}}{3} \int_0^{\eta_0} d\eta e^{-\tau} \beta_l^{(1)}(k(\eta_0 - \eta)) \mathcal{T}(k, \eta)$$

$$= -\frac{\sqrt{(l-1)(l+1)}}{3\sqrt{2}} \int_0^{\eta_0} d\eta \frac{j_l(k(\eta_0 - \eta))}{\eta_0 - \eta}$$

$$\times \mathcal{T}(k, \eta) e^{-\tau}. \quad (\text{A25})$$

As a first step, let us assume that the velocity field is simply being red-shifted by the expansion of the universe. Then

$$\mathcal{T}(k, \eta) = \left( \frac{a_{rec}}{a} \right)^2. \quad (\text{A26})$$

For small  $l$  we can evaluate  $C_l^{TB}$  and  $C_l^{EB}$  approximately, assuming  $g(k) = 1$ :

$$\tilde{\Delta}_l(k) \approx \sqrt{\frac{l(l+1)}{2}} \frac{j_l(k\eta_0)}{k\eta_0}, \quad (\text{A27})$$

$$\tilde{E}_l(k) \approx \frac{\sqrt{(l-1)(l+1)}}{3\sqrt{2}} \frac{j_l(k\eta_0)}{k\eta_0} \left[ 1 + 2 \left( \frac{\dot{a}}{a\dot{\tau}} \right)_{rec} \right], \quad (\text{A28})$$

$$\tilde{B}_l(k) \approx -\frac{\sqrt{(l-1)(l+1)}}{3\sqrt{2}} \frac{j_l(k\eta_0)}{\eta_0} \dot{\tau}_{rec}^{-1}, \quad (\text{A29})$$

$$C_l^{TB} = \frac{(l+1)\sqrt{l(l-1)}}{3\pi} \frac{v_0^2}{\dot{\tau}_{rec}\eta_0} (k_*\eta_0)^{-(n+3)} \times \int_0^\infty dx x^{n+1} j_l^2(x), \quad (\text{A30})$$

$$C_l^{EB} = -\frac{(l-1)(l+1)}{9\pi} \frac{v_0^2}{\dot{\tau}_{rec}\eta_0} (k_*\eta_0)^{-(n+3)} \times \left[ 1 + 2 \left( \frac{\dot{a}}{a\dot{\tau}} \right)_{rec} \right] \int_0^\infty dx x^{n+1} j_l^2(x). \quad (\text{A31})$$

The last integral can be evaluated:

$$\int_0^\infty dx x^{n+1} j_l^2(x) = \frac{2^{n-1}\pi\Gamma(-n)\Gamma(l+1+\frac{n}{2})}{\Gamma^2(\frac{1-n}{2})\Gamma(l+1-\frac{n}{2})}. \quad (\text{A32})$$

We find for  $n < 0$  that

$$C_l^{TB,EB} \propto l^{n+2}. \quad (\text{A33})$$

For  $n \geq 0$  the integral diverges and is dominated by the range near the cutoff:

$$\int_0^{x_0} dx x^{n+1} j_l^2(x) \sim \frac{x_0^{n+2}}{n+1} \quad (\text{A34})$$

and  $C_l^{TB,EB} \propto l^2$ .

The expressions in Eqs. (A21) and (A22) have been evaluated numerically and the results are described in Sec. II.

## APPENDIX B

Here we find the vorticity induced by magnetic fields at last scattering in the two-fluid approximation where the photon and electron velocities are equal, but the proton velocities can be different. This is closely analogous to Harrison's calculation of the induced magnetic field due to cosmic vorticity [11].

The starting point is the Euler flow equations for the velocities  $\mathbf{v}_b$ ,  $\mathbf{v}_e$ ,  $\mathbf{v}_\gamma$  of the baryon (*i.e.* proton), electron and photon fluids. These equations are all of the form

$$\rho_i \frac{d\mathbf{v}_i}{dt} = \mathbf{F}_i - \sum_{j \neq i} \mathbf{P}_{ij}, \quad (\text{B1})$$

where

$$\frac{d\mathbf{v}}{dt} = \frac{\partial \mathbf{v}}{\partial t} + (\mathbf{v} \cdot \nabla) \mathbf{v} \quad (\text{B2})$$

is the total derivative of the velocity,

$$\mathbf{F}_i = n_i Z_i e (\mathbf{E} + \mathbf{v}_i \times \mathbf{B}) \quad (\text{B3})$$

is the force from the electromagnetic field per unit volume,  $Z_i e$  is the charge of particles constituting the fluid  $i$ , and  $\mathbf{P}_{ij} = -\mathbf{P}_{ji}$  is the rate of momentum transfer to the fluid  $i$  due to collisions with the fluid  $j$  [hence the

negative sign in Eq. (B1)] per unit volume. For baryons we take  $Z_b = +1$ . We can also add a gradient of the gravitational potential  $\nabla\phi$  to the equation for baryons. The density of particles is  $\rho_i = n_i m_i$ .

Collisions between photons and baryons are disregarded because they transfer much less momentum than collisions between other fluids. Collisions of electrons with baryons determine the conductivity  $\sigma$  of the plasma:

$$\mathbf{P}_{eb} = \frac{en_e}{\sigma} \mathbf{j}. \quad (\text{B4})$$

The velocities  $\mathbf{v}_i$  of the fluids are almost equal to each other due to tight coupling, however the velocities of electrons and photons are closer to each other than the velocities of electrons and baryons:

$$|\mathbf{v}_\gamma - \mathbf{v}_e| \ll |\mathbf{v}_e - \mathbf{v}_b| \ll \mathbf{v}_b. \quad (\text{B5})$$

We take the velocities of the electrons and photons to be the same, except when computing  $\mathbf{P}_{e\gamma}$ .

We now rewrite the Euler flow equations for baryons electrons, expressing the combination  $\mathbf{E} + \mathbf{v}_i \times \mathbf{B}$  through other quantities:

$$\mathbf{E} + \mathbf{v}_b \times \mathbf{B} = \frac{m_b}{e} \left( \frac{d\mathbf{v}_b}{dt} + \nabla\phi \right) + \frac{1}{\sigma} \mathbf{j}, \quad (\text{B6})$$

$$\mathbf{E} + \mathbf{v}_e \times \mathbf{B} = -\frac{m_e}{e} \frac{d\mathbf{v}_e}{dt} + \frac{1}{\sigma} \mathbf{j} - \frac{1}{en_e} \mathbf{P}_{e\gamma}. \quad (\text{B7})$$

The flow equation for photons is

$$(\rho_\gamma + p_\gamma) \frac{d\mathbf{v}_\gamma}{dt} + \mathbf{v}_\gamma \frac{dp_\gamma}{dt} = -(\rho_\gamma + p_\gamma) \nabla\phi - \mathbf{P}_{e\gamma}, \quad (\text{B8})$$

and we use the equation of state  $p_\gamma = \rho_\gamma/3$ .

Maxwell's equations in the MHD approximation are

$$\nabla \times \mathbf{E} = -\frac{\partial \mathbf{B}}{\partial t}, \quad \nabla \times \mathbf{j} = -\nabla^2 \mathbf{B}. \quad (\text{B9})$$

Taking curl of Eq. (B6), using  $\nabla \cdot \mathbf{B} = 0$  and Eq. (B2) for the total derivative  $d/dt$ , we obtain

$$\frac{e}{m_b \sigma} \nabla^2 \mathbf{B} = \frac{e}{m_b} \left[ \frac{d\mathbf{B}}{dt} + \mathbf{B} (\nabla \cdot \mathbf{v}_b) - (\mathbf{B} \cdot \nabla) \mathbf{v}_b \right] + \nabla \times [(\mathbf{v}_b \cdot \nabla) \mathbf{v}_b] - (\mathbf{v}_b \cdot \nabla) \boldsymbol{\omega}_b + \frac{d\boldsymbol{\omega}_b}{dt}. \quad (\text{B10})$$

Next we write

$$\mathbf{v}_b = \mathbf{u} + \mathbf{w}, \quad (\text{B11})$$

where  $\mathbf{u} = \dot{R}\mathbf{r}/R$  is the velocity due to Hubble expansion,  $R(t)$  is the universal scale factor, and  $\mathbf{w}$  is the vortical velocity in the angular direction around the line of vorticity which is taken to coincide with the direction of the magnetic field lines (assumed to be parallel). Then, after some manipulations, we obtain

$$\frac{m_b}{e} \left( \frac{d\boldsymbol{\omega}_b}{dt} + 2\boldsymbol{\omega}_b \frac{\dot{R}}{R} \right) + \frac{d\mathbf{B}}{dt} + 2\mathbf{B} \frac{\dot{R}}{R} = \frac{1}{\sigma} \nabla^2 \mathbf{B}. \quad (\text{B12})$$

We can rewrite this as

$$\frac{d}{dt} \left( \frac{m_b}{e} \boldsymbol{\omega}_b R^2 + \mathbf{B} R^2 \right) = \frac{R^2}{\sigma} \nabla^2 \mathbf{B}. \quad (\text{B13})$$

In Eq. (B7), Harrison neglects the  $d\mathbf{v}_e/dt$  terms and also takes  $\mathbf{v}_e = \mathbf{v}_\gamma$  in the  $\mathbf{v}_e \times \mathbf{B}$  term. Taking curl of that equation then gives

$$\frac{d\mathbf{B}}{dt} + 2\mathbf{B} \frac{\dot{R}}{R} = -\frac{1}{en_e} \nabla \times \mathbf{P}_{e\gamma} + \frac{1}{\sigma} \nabla^2 \mathbf{B}. \quad (\text{B14})$$

(Harrison also neglects the  $\nabla^2 \mathbf{B}$  term which we keep here.) The unknown quantity  $\nabla \times \mathbf{P}_{e\gamma}$  in Eq. (B14) is found by taking the curl of Eq. (B8),

$$4\rho_\gamma \left( \frac{d\boldsymbol{\omega}_\gamma}{dt} + \boldsymbol{\omega}_\gamma \frac{\dot{R}}{R} \right) = -3\nabla \times \mathbf{P}_{e\gamma}. \quad (\text{B15})$$

Combining Eqs. (B14) and (B15), we get

$$\frac{d\mathbf{B}}{dt} + 2\mathbf{B} \frac{\dot{R}}{R} = \frac{4}{3} \frac{1}{en_e} \rho_\gamma \left( \frac{d\boldsymbol{\omega}_\gamma}{dt} + \boldsymbol{\omega}_\gamma \frac{\dot{R}}{R} \right) + \frac{1}{\sigma} \nabla^2 \mathbf{B}. \quad (\text{B16})$$

Note that  $\rho_\gamma(t) = \rho_\gamma^{(0)} R^{-4}$  and  $\rho_e(t) = \rho_e^{(0)} R^{-3}$ . Multiplying Eq. (B16) by  $R^2$  and rewriting it as a total time derivative,

$$\frac{d}{dt} \left[ \mathbf{B} R^2 - \frac{4m_e \rho_\gamma^{(0)}}{3e \rho_e^{(0)}} \boldsymbol{\omega}_\gamma R \right] = \frac{R^2}{\sigma} \nabla^2 \mathbf{B}. \quad (\text{B17})$$

Subtracting Eq. (B17) from Eq. (B13) and integrating with the initial condition of zero vorticity finally gives:

$$\frac{m_b R^2}{e} \boldsymbol{\omega}_b = -\frac{4\rho_\gamma^{(0)} m_e R}{3e \rho_e^{(0)}} \boldsymbol{\omega}_\gamma. \quad (\text{B18})$$

Additionally, we take the curl of

$$\mathbf{v}_b - \mathbf{v}_e = \frac{1}{en_e} \mathbf{j}, \quad (\text{B19})$$

equate  $\boldsymbol{\omega}_\gamma$  and  $\boldsymbol{\omega}_e$ , and obtain

$$\boldsymbol{\omega}_b - \boldsymbol{\omega}_\gamma = -\frac{1}{en_e} \nabla^2 \mathbf{B}. \quad (\text{B20})$$

Now we have two simultaneous equations, Eq. (B18) and (B20) for the two vorticities  $\boldsymbol{\omega}_e = \boldsymbol{\omega}_\gamma$  and  $\boldsymbol{\omega}_b$ . Recognizing that  $\rho_\gamma \ll \rho_b$  at last scattering, we then solve the simultaneous equations to get

$$\boldsymbol{\omega}_e = \frac{1}{en_e} \nabla^2 \mathbf{B}. \quad (\text{B21})$$

- 
- [1] E. S. Scannapieco and P. G. Ferreira, Phys. Rev. **D56**, 7493 (1997).
  - [2] A. Lue, L. Wang, and M. Kamionkowski, Phys. Rev. Lett. **83**, 1506 (1999).
  - [3] G. B. Field and S. M. Carroll, Phys. Rev. **D62**, 103008 (2000).
  - [4] J. M. Cornwall, Phys. Rev. **D56**, 6146 (1997).
  - [5] T. Vachaspati, Phys. Rev. Lett. **87** 251302 (2001).
  - [6] T. Vachaspati, astro-ph/0111124, to be published in the proceedings of the Cosmo-01 workshop (2001).
  - [7] S. Chandrasekhar, *Radiative Transfer*, Dover, New York (1960).
  - [8] A. Kosowsky, Ann. Phys. **246**, 49 (1996).
  - [9] W. Hu and M. White, Phys. Rev. **D56**, 596 (1997).
  - [10] U. Frisch, A. Pouquet, J. Leorat, and A. Mazure, J. Fluid Mech. **68**, 769 (1975).
  - [11] E. R. Harrison, Mon. Not. R. Astr. Soc. **147**, 279 (1970).
  - [12] D. D. Harari, J. D. Hayward, and M. Zaldarriaga, Phys. Rev. **D55** (1997).
  - [13] A. Kosowsky and A. Loeb, Ap. J. **469**, 1 (1996).
  - [14] T. R. Seshadri and K. Subramanian, Phys. Rev. Lett. **87**, 101301 (2001).